Desalination and Water Treatment
www.deswater.com

doi:10.5004/dwt.2018.22915

124 (2018) 297–307
August

Adsorption behavior of methylene blue on acid-treated rubber (*Hevea brasiliensis*) leaf

Ali H. Jawad[a,*], Shaimaa Hassan Mallah[b], Mohd Sufri Mastuli[a]

[a]*Faculty of Applied Sciences, Universiti Teknologi MARA, 40450 Shah Alam, Selangor, MALAYSIA, Tel. +603-55211721, email: ahjm72@gmail.com, ali288@salam.uitm.edu.my (A.H. Jawad), Tel. + 03 5543 6594, email: mohdsufri@salam.uitm.edu.my (M.S. Mastuli)*
[b]*Department of Chemistry, College of Science, ALMuthanna University, IRAQ, Tel. +9647804611780, email: Shaimaa.h2m30@yahoo.com (S.H. Mallah)*

Received 5 November 2017; Accepted 6 August 2018

ABSTRACT

The rubber (*Hevea brasiliensis*) leaf is an agricultural waste was chemically treated with H_2SO_4 to be a potential biochar adsorbent for methylene blue (MB) adsorption from aqueous solution. The acid-treated rubber leaf (ATRL) was characterized by a CHNS-O, Brunauer-Emmett-Teller (BET), X-ray diffraction (XRD), Fourier transform infrared spectroscopy (FTIR), scanning electron microscope with an energy dispersive X-ray spectrometer (SEM-EDX), *point-of-zero charge* (pH_{PZC})and proximate analyses. Batch mode adsorption studies were conducted by varying operational parameters such as adsorbent dosage (0.02–0.30 g), solution pH (3–11), initial MB concentrations (50–300 mg/L) and contact time (0–1440 min). The equilibrium data were well fitted to Freundlich isotherm compare to Langmuir and Temkin isotherms. The maximum adsorption capacity, q_{max} of ATRL for MB adsorption was 263.2 mg/g at 303 K. The kinetic uptake profiles were well described by the pseudo-second-order model. The thermodynamic adsorption parameters such as standard enthalpy (ΔH°), standard entropy (ΔS°), and standard free energy (ΔG°) showed that the adsorption of MB onto ATRL surface endothermic in nature and spontaneous under the experimented conditions. All results mentioned above revealed that the ATRL can be feasibly utilized for the removal of MB from aqueous solution.

Keywords: Rubber leaf; Acid-treated; Chemical activation; Sulphuric acid; Adsorption; Methylene blue

1. Introduction

Number of industries such as textile, rubber, paper, plastics, leather and food uses dyes to colour their products while residual unspent dyes are settled into the rivers and other natural water bodies. The discharge of dye-contained wastewaters into ecosystem is a dramatic source of aesthetic pollution, eutrophication and perturbation in aquatic life as most of dyes are highly visible, stable and unaffected to chemical, photochemical as well as biological degradation [1–3]. Basic dyes are cationic species originating from positively charged nitrogen or sulphur atoms. In fact, basic dyes are named because of their affinity to basic textile materials with net negative charge [4]. Methylene blue (MB) is a basic dye with favourable water solubility and the most commonly used dye in industrial applications such as dyeing of textiles and leather, printing calico, printing cotton and biological staining methods [5]. MB is chosen to represent a group of dyes, which are commonly large in molecular size and difficult to be degraded in natural environment. Tinctorial value of MB is very high, in spite of low toxicity (<1 mg/L) a noticeable coloration is detected and can be classified as toxic colorants [6]. MB is reported to result in harmful effects such as eye irritation, gastrointestinal irritation and nausea upon ingestion, including vomiting and diarrhea [7]. Removal of MB from wastewater is a major environmental challenge and there is a continuous need to have an effective process that can efficiently remove it economically.

*Corresponding author.

There are many useful methods have been applied for dyes removal from industrial effluents and wastewaters such as Bioremediation [8], electrochemical degradation [9], cation exchange membranes [10], Fenton chemical oxidation [11] and photocatalysis [12,13]. Most of these methods have techno-economical limitations for field-scale applications [14]. Comparatively, adsorption has been proved to be a well-established and most widely used technique among other water purification processes. This technique is effective in removing suspended solids, odours, organic matter and oil from aqueous solutions. Adsorption-based treatment with appropriate adsorbent materials shows high performance and selectivity, flexibility and simplicity of design, convenience of operation without producing harmful by-products as well as economically cost effective [15].

Activated carbon (AC) is referred as carbonaceous materials [16], with high porosity [17–21], high physicochemical stability [22], high adsorptive capacity [23], high mechanical strength [24,25], high degree of surface reactivity [26,27], with immense surface area [28,29] which can be differentiated from elemental carbon by the oxidation of the carbon atoms that found at the outer and inner surfaces [30]. Therefore, AC has been widely utilized in versatile applications such as gas separation, solvents recovery, gas storage, super capacitors electrodes, catalyst support, adsorbent for organic and inorganic pollutants from drinking water, and so on [31]. However, a high cost of AC production limits its application in various technologies. Recognizing this economic obstacle, many investigators have been made extensive efforts in low-cost alternatives to AC from a range of carbonaceous precursors, such as ligno-cellulosic materials [32], biopolymer [33], coal [34], char [35], and fruit peels [36]. The textural properties and adsorption capacities of AC aremainly depend on the nature of the starting martial, activation method, and type of activator and preparation conditions [37].

Chemical surface modification methods are widely used to prepare hydrophilic carboneous materials and biochar. Hydrophilicity of the carboneous materials is associated essentially with the presence of oxygen containing groups on the surface such as carboxylic, phenolic and lactonic groups. Sulphuric acid is a reagent frequently used to enhance oxygen content on the surface [38]. Researches demonstrated that the amount of oxygen containing surface functional groups, specific surface area and pore structure highly depend on the concentration of activation agents. While oxygen content of carboneous materials usually increases with the increase of reagent concentration, the surface area and pore volume values decrease adversely [39]. Nowadays, interests are growing in the utilizing of agricultural waste and food residues as low-cost and steady sources for the developing rich carboneous materials with multifunctional functional groups that can be potentially for removal of water pollutants.

Rubber (*Hevea brasiliensis*) tree is widely planted in Malaysia and become one of the major plantation crops other than oil palm. The tree is cultivated in large commercial scale in several countries in the tropics amounting to 9.485 million ha worldwide [40]. Since rubber related industries are expanding to meet demands from consumers, the economic importance of the rubber tree has largely focused on the rubber latex with little attention paid to the potential usefulness of its by-product. Rubber plantation in Malaysia generates a huge amount of waste rubber leaf (RL) especially during dry season (February to March) every year.

Therefore, the main objectives of this work were: firstly to make better utilization of this abundant agricultural waste (RL) to be a promising precursor for developing renewable biochar by using one-step treatment with sulphuric acid (H_2SO_4) as a chemical activator; Secondly, to investigate the adsorption behavior of MB removal from aqueous solution, with the long-term target of applying such renewable carboneous biochar adsorbents to wastewater treatment processes in the textile industry. In fact, the role of H_2SO_4 is to create several oxygen complexes and improving the surface porosities through modification of biochar with liquid concentrated H_2SO_4 at relatively low temperature. Thus, MB was chosen as a typical cationic dye to figure out the adsorptive properties of the ATRL. Moreover, sulphuric acid (H_2SO_4) is frequently used as a low cost chemical agent for the preparation of carboneous adsorbents from ligno-cellulosic materials such as coconut leaf [32], mango peel [36], *euphorbia rigida* [41], bagasse [42], almond husk [43], *parthenium hysterophorus* [44], sunflower oil cake [45], pine-fruit shell [46], *Delonix regia*pods [28], wild carrot [47], *Ficuscarica* [48] potato peel and neem bark [49].

2. Materials and methods

2.1. Adsorbate (MB)

The cationic dye, methylene blue (MB) was used as an adsorbate in this work. MB was purchased from R&M Chemicals, Malaysia with chemical formula ($C_{16}H_{18}ClN_3S{\cdot}xH_2O$) and molecular weight (319.86 g/mol). Ultra-pure water was used to prepare all solutions.

2.2. Preparation and characterization of ATRL

The rubber leaf (RL) was collected from a rubber plantation estate in Pauh, Perlis, Malaysia and was used as the precursor for the preparation of biochar in this work. The RL was first washed with water to remove dirt and subsequently dried at 105°C for 24 h to remove the moisture contents. The dried RL was ground and sieved to the size of 250–500 μm before mixing with concentrated H_2SO_4 (95–98%). The mixing ratio was fixed at 1 g of dried RL powder with 1 mL of concentrated H_2SO_4 according to the method reported by Garg et al. [50]. The acid-treated rubber leaf (ATRL) was washed with hot distilled water until the filtrate water was clear and reached a neutral pH value. The elemental analysis was carried out using a CHNS-O analyser (Flash 2000, Organic Elemental Analyzer, Thermoscientific). The oxygen contents were calculated by difference. X-ray diffraction analysis (XRD) was performed by X-ray diffraction (XRD) in reflection mode (Cu Kα radiation) on a PANalytical, X'Pert Pro X-ray diffractometer. Scans were recorded with a scanning rate of 0.59°/s. The diffraction angle (2θ) was varied from 10° to 90°. Textural characterization of ATRL was carried out by N_2 adsorption using Micromeritics ASAP 2060, USA. FT-IR spectral analysis of ATRL was performed on a Perkin Elmer, Spectrum One in

the 4000 cm^{-1}–500 cm^{-1} wavenumber range. The surface physical morphology was examined by using scanning electron microscopy (SEM; SEM-EDX, FESEM CARL ZEISS, SUPKA 40 VP). The pH at the *point-of-zero charge* (pH_{PZC}) was estimated using a pH meter (Metrohm, Model 827 pH Lab, Switzerland), as described elsewhere [51].

2.3. Batch adsorption experiments

The batch adsorption experiments of MB adsorption onto ATRL surface were performed in a set of 250 mL Erlenmeyer flasks containing 100 mL of MB solution. The flasks were capped and agitated in an isothermal water bath shaker (Memmert, waterbath, model WNB7-45, Germany) at fixed shaking speed of 110 stroke/min and 303 K until equilibrium was achieved. Batch adsorption experiments were carried out by varying several experimental variables such as adsorbent dosage (0.02–0.3 g), pH (3–11), initial dye concentration (50–300 mg/L) and contact time (0–1440 min.) to determine the best uptake conditions for MB adsorption. The pH of MB solution was adjusted by adding either 0.1 mol/L HCl or NaOH. After mixing of the ATRL-MB system, the supernatant was collected with a 0.20 μm Nylon syringe filter and the concentrations of MB were monitored at a different time interval using a HACH DR 2800 Direct Reading Spectrophotometer at the maximum wavelength (λ_{max}) of absorption at 661 nm. For the thermodynamic studies, the same procedures were repeated and applied at 313 K, 323 K and 333 K with the other parameters keep constant. The blank test was carried out in order to account for colour leached by the adsorbent and adsorbed by the glass containers, blank runs with only the adsorbent in 100 mL of doubly distilled water and 100 mL of dye solution without any adsorbent were conducted simultaneously at similar conditions. The adsorption capacity at equilibrium, q_e (mg/g) and the percent of colour removal, CR (%) of MB were calculated using Eqs. (1) and (2).

$$q_e = \frac{(C_o - C_e)V}{W} \tag{1}$$

$$CR\,\% = \frac{(C_o - C_e)}{C_o} \times 100 \tag{2}$$

where C_o and C_e (mg/L) are the initial and equilibrium concentrations of MB, respectively, V (L) is the volume of the solution and W (g) is the mass of dry adsorbent used.

3. Results and discussion

3.1. Characterization of ATRL

3.1.1. Physical properties

The results of physical characterization of ATRL are recorded in Table 1. The ultimate results indicate that ATRL has a relatively high carbon content (53.45%), oxygen content (40.04%), and sulphur (0.55) with low surface area (1.65 m^2/g). The low surface area of ATRL can be attributed to the high concentration of activation agent H_2SO_4, which basically responsible for increasing the oxygen content and detected sulphur on ATRL surface and decreasing adversely the surface area and pore volume [39].

Table 1
Characterization in contents of ATRL

Proximate analysis	Values
Bulk density g/mL	0.63
Ash content (wt %)	6.91
Moisture content (wt %)	9.59
Fixed carbon, %	66.36
Elemental analysis (wt. %)	**Values**
Carbon, C	53.45
Hydrogen, H	4.38
Nitrogen, N	1.58
Sulphur, S	0.55
Oxygen, O (by difference)	40.04
Surface area analysis	**Values**
Total pore volume (cm^3/g)	0.00342
Mean pore width (nm)	48.60
BET surface area (m^2/g)	1.65

3.1.2. XRD analysis of ATRL

The XRD pattern of the ATRL is shown in Fig. 1. XRD pattern is indexed based on a standard diffraction reference pattern (PCPDF No: 898487). Appearance of a broad diffraction background and the absence of a sharp peak reveal a predominantly amorphous structure [52]. Overall, there were two XRD peaks at 2θ = 22° (002) and 2θ = 42° (101) in the spectrum. These signatures relate to crystalline carbon with expanded lattice parameters (carbon with impurities).

3.1.3. FTIR spectral analysis

FTIR spectral analysis provides structural and compositional information on the active functional groups presented in the ATRL. FTIR spectrum of ATRL before adsorption (Fig. 2a) shows various functional groups, in agreement with their respective wavenumber (cm^{-1}) position as reported in literature. The broad band observed ~3500 cm^{-1} is assigned to the stretching vibrations of the hydroxyl (O-H) [53]. The band at ~1700 cm^{-1} associated to C=O stretching of ketones, aldehydes, lactones or carboxyl groups, and the band at 1600 cm^{-1}–1580 cm^{-1} is assigned to C=C vibrations in aromatic rings [7]. The absorptions peaks between 1300 $cm^{-1}$and 1000 cm^{-1} are observed for oxidized carbon materials and are assigned to C–O and/or C–O–C stretching in acids, alcohols, phenols, ethers and/or esters groups and sulphonic acid groups (–SO_3) [32,52,53]. Thus, the FTIR spectrum of ATRL before adsorption indicates that the external surface of ATRL is rich-SO_3H group in addition to various functional groups, containing oxygen of carboxylic and carbonyl species. These active groups on ATRL surface are responsible for enhancing the adsorption of cationic species such as MB due to the electrostatic interaction. After MB adsorption (Fig. 2b), some of the bands shifted and became more pronounced in which the attenu-

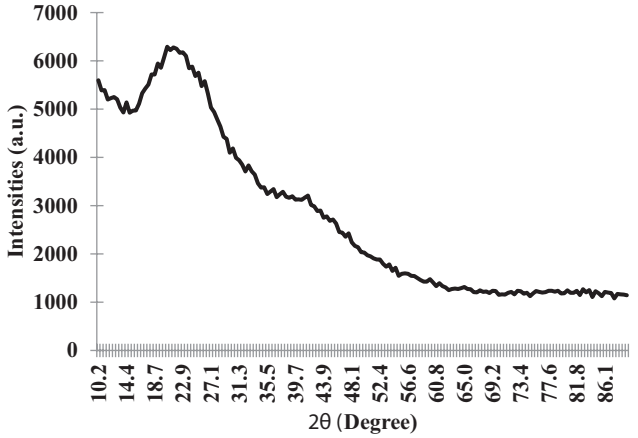

Fig. 1. XRD pattern of ATRL.

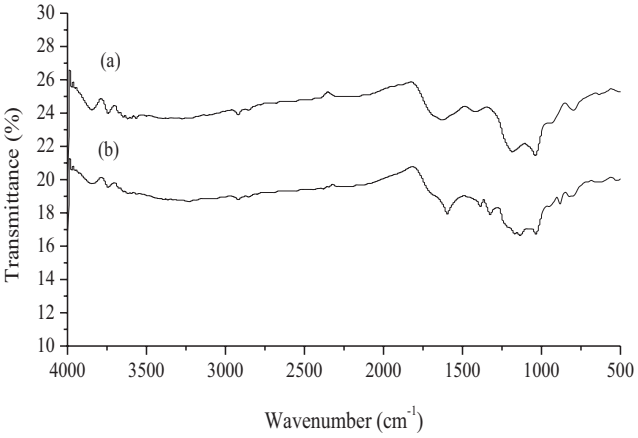

Fig. 2. FTIR spectra of ATRL: (a) before MB adsorption, and (b) after MB adsorption.

ated bands at ~1650 cm^{-1} (–N–H bending), ~1380 cm^{-1} (C–N bending vibration) and ~850 cm^{-1} (–CH_2 vibration) suggest the interaction of MB molecules with the functional groups of ATRL.

3.1.4. SEM-EDX analysis

SEM images were recorded to visualize the surface physical morphology of ATRL. The SEM and EDX results of ATRL before and after adsorption are shown in Figs. 3a and 3b, respectively. As can be seen in Fig. 3a, the surface of ATRL appears to be highly porous and heterogeneous with tunnel or honeycomb-like structures. Pores with different size and shape are also clearly visible. Those pores are pitted and fragmented due to evaporation of the H_2SO_4 during carbonization, leaving the space being previously occupied by the reagent. In Fig. 3a also, EDX analysis reconfirm that ATRL sample has high content of carbon (69.71%), oxygen (29.46%), and little sulphur (0.83%). The presence of sulphur as (–SO_3H) group in the structure of ATRL can be attributed to the role of the strong chemical activator (H_2SO_4). In fact, development such a rich –SO_3H group on the surface of ATRL plus porous structure may be highly favourable for the uptake of cationic species like MB dye *via* electrostatic interaction. Therefore, this unique property of ATRL surface can strongly attract MB molecules from aqueous solution. After MB adsorption (Fig. 3b), the ATRL surface is altered to be more compact and less open pores are seen due to loading of MB molecules on the ATRL surface. Additionally, the corresponding EDX analysis indicates that the ATRL surface consists of mainly C, O, and S. The higher content of C in the EDX analysis after MB adsorption can be attributed to the MB molecules attached onto ATRL surface.

3.1.5. Point-of-zero charge (pH_{PZC})

Based on the precursor origin and the preparation mode, AC can possess acidic, basic or neutral nature (amphoteric). The *point-of-zero charge* (pH_{PZC}) test estimates the pH at which the net charge of the surface is zero. Fig. 4 shows the pH_{PZC} result of the experiment performed with the ATRL, where the pH ranged from 3 to 11. The pH_{PZC} of the ATRL was 5.2, which indicates the acid character of the ATRL surface, in agreement with the presence of acid groups from the FTIR results (Fig. 2a). In general, the adsorption of anions is favoured at solution pH below the pH_{PZC} value as the surface of ATRL is positively charged due to protonation whereas at solution pH above the pH_{PZC} value, the surface of ATRL becomes negatively charged and thus, adsorption of cations is preferred. In this respect, Jawad et al., reported that the pH_{PZC} values of the coconut leaf and mango peel treated with H_2SO_4 were 3.20 [32] and 4.60 [36] for, respectively. Furthermore, Karagöz et al., [45] reported that the pH_{PZC} value lies between pH 2.5 and 5.5 which was attributed to the acid form of AC derived from sunflower oil cake treated with H_2SO_4.

3.2. MB adsorption

3.2.1. Effect of the adsorbent dosage

Adsorbent dosage shows a profound effect on the adsorption process, due to the reason that it predicts the cost of pollutant to be treated. The effect of adsorbent dosage on the removal of the MB from aqueous solution was determined using variable quantities of ATRL adsorbent ranging from 0.02 to 0.30 g at fixed volumes (100 mL) and initial dye solution where C_o was 100 mg/L. For these experiments, other operation parameters were held constant at 303 K, shaking speed of 110 stroke/min, contact time of 180 min, and an unadjusted pH at 5.60 for the initial MB solution. The effect of adsorbent dosage on the adsorptive removal of MB is displayed in Fig. 5. It is apparent that the highest level of MB removal was achieved using 0.10 g ATRL and thereafter, further increase in adsorbent dosage did not exert an appreciable increase in the MB removal percentage. The observed increase in the dye removal (%) with adsorbent dosage was attributed to an increased in the adsorbent surface area, which increased the availability of more adsorption sites. However, no significant changes in MB removal efficiency were observed beyond 0.10 g/100 mL ATRL dose. Therefore, in the further experiments the adsorbent dosage was fixed at 0.10 g.

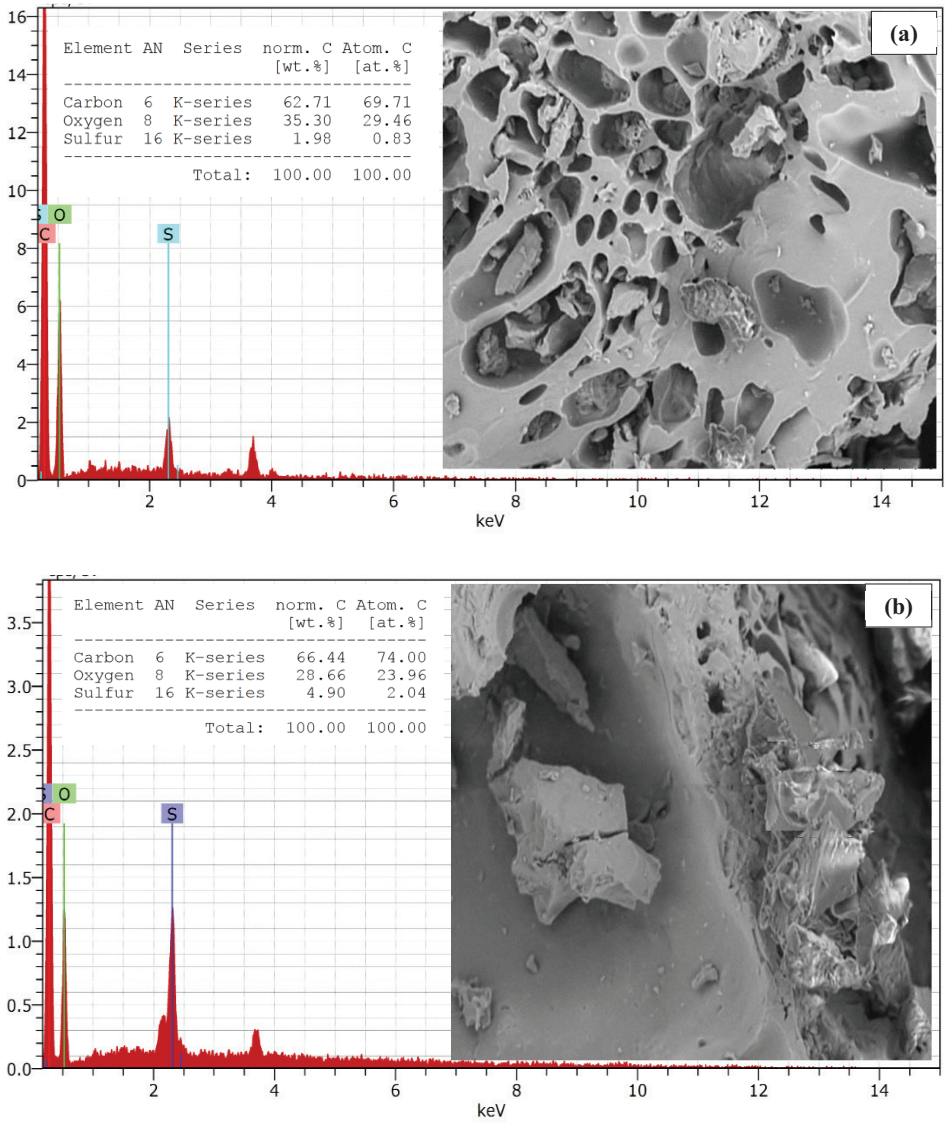

Fig. 3. Typical SEM micrograph of ATRL particle (2.0 kx magnifications): (a) before MB adsorption and (b) after MB adsorption.

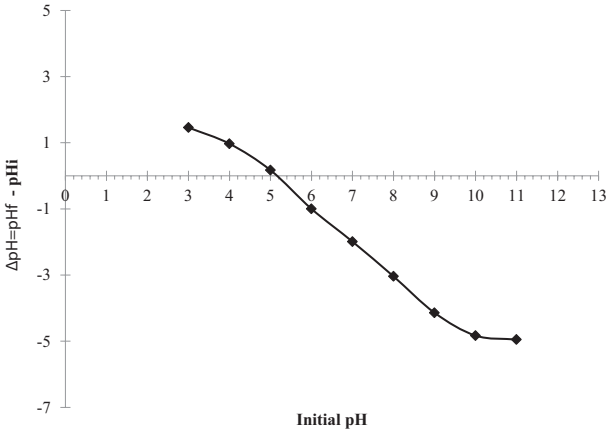

Fig. 4. pHpzc of ATRL suspensions.

3.2.2. *Effect of pH*

The pH of the solution influences the speciation of the dyes, along with the surface charge of the adsorbent. Fig. 6 shows the effect of variable pH from 3 to 11 on the adsorption capacity with MB. However, MB uptake (q_e) onto ATRL was not affected by pH within the studied range from due to buffering effect of the adsorbent [54]. Similar observations had been reported for the adsorption of MB by coconut leaf [7,32,55], *Parthenium hysterophorus* [44], *Prosopis cineraria sawdust* [50] and *Posidonia oceanica (L.)* fibers [56]. In general, at lower pH, the surface charge may be positively charged, thus making (H^+) ions compete effectively with dye cations causing a decrease in the amount of dye adsorbed. At higher pH values, the surface of AC adopts a negative surface charge, which contributes to enhanced uptake of positively charged dye species via attractive electrostatic attraction, in accordance with an increase in the

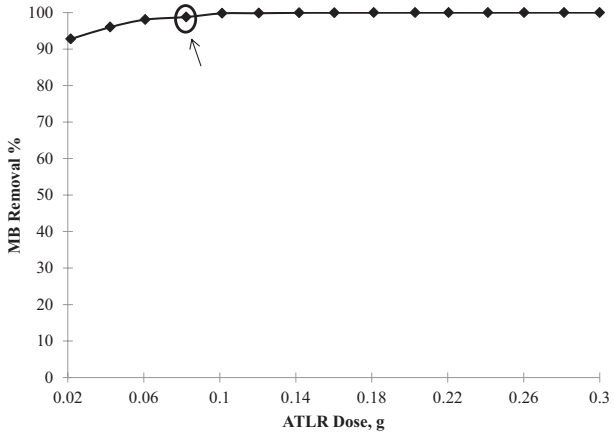

Fig. 5. Effect of ATRL dosage on MB removal (%) at [MB]o = 100 mg/L, V = 100 mL, pH = 5.6, T = 303 K, shaking speed = 110 stroke/min and contact time = 180 min.

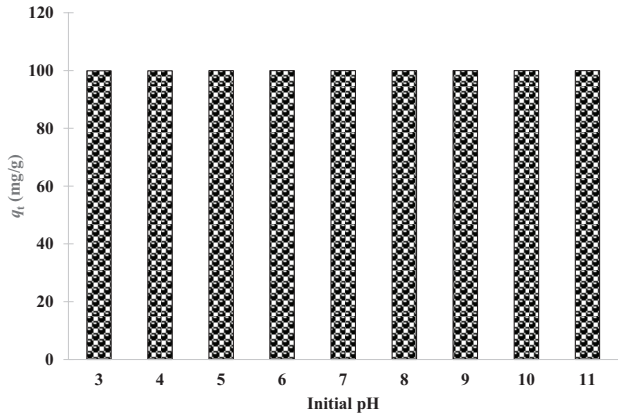

Fig. 6. Effect of pH on the adsorption capacity of MB by ATRL at [MB]o = 100 mg/L, V = 100 mL, T = 303 K, shaking speed = 110 stroke/min, contact time = 180 min and ATRL dosage = 0.1 g.

rate of adsorption [57]. To continue this work, the effective pH for ATRL was fixed at 5.6, and used in further adsorption studies herein.

3.2.3. Effect of initial dye concentration and contact time

The adsorption efficiency of MB on ATRL was evaluated as a function of initial concentrations and contact time are shown in Fig. 7. The amount of MB adsorbed by the ATRL adsorbent at equilibrium enhance rapidly from 50.4 mg/g to 268.2 mg/g as the initial dye concentration increased from 50 to 300 mg/L. This increase is mainly determined by the fact that the high initial MB concentration not only provides a large driving force to overcome all mass transfer resistances between the aqueous and solid phases, but also determines a higher probability of collision between MB ions and ATRL surface. Additional time was needed to reach equilibrium for higher dye concentration because there was a tendency for MB to penetrate deeper within the interior surface of the ATRL and be adsorbed at active pore sites. This indicates that the initial dye concentration plays a

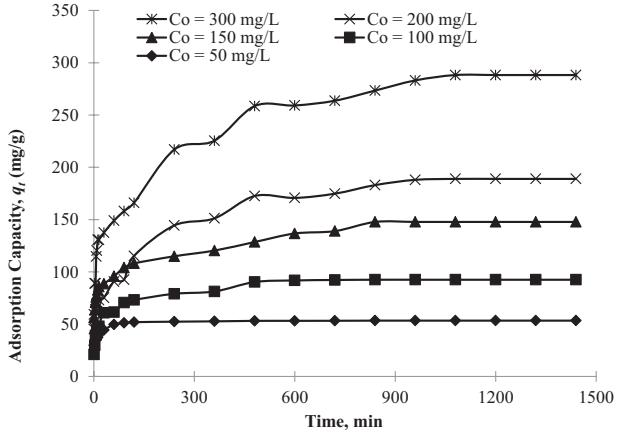

Fig. 7. Effect of initial concentration and contact time on the adsorption of MB by ATRL (V = 100 mL, T = 303 K, pH = 5.6, shaking speed = 110 stroke/min and ATRL dosage = 0.1 g).

significant role in the adsorption capacity of MB onto ATRL sorbent.

3.3. Adsorption isotherm

The application of adsorption isotherm is very useful to describe the interaction between the adsorbate and the adsorbent of any system [51]. The parameters obtained from the different models provide important information on the sorption mechanisms, surface properties and affinities of the adsorbent. In this work, the adsorption isotherm results for ATRL were fitted using most accepted surface adsorption models for single solute systems, which are Langmuir, Freundlich, and Temkin model. Langmuir model is based on the assumption that adsorption occurs at specific homogenous sites within the adsorbent [58]. It explains monolayer adsorption which lies on the fact that the adsorbent has a finite number of adsorption sites of uniform strategies of adsorption with no transmigration of adsorbate in the plane of surface, i.e. at equilibrium; a saturation point is attained where no further adsorption can occur. Eq. (3) shows the Langmuir isotherm expressions:

$$\frac{C_e}{q_e} = \frac{1}{q_{\max} k_L} + \frac{1}{q_{\max}} C_e \tag{3}$$

where C_e is the equilibrium concentration (mg/L) and q_e is the amount of adsorbed species per specified amount of adsorbent (mg/g), k_L is the Langmuir equilibrium constant and q_{max} is the amount of adsorbate required to form an adsorbed monolayer. Hence, a plot of C_e/q_e vs. C_e should be a straight line with a slope ($1/q_{max}$) and an intercept ($1/q_{max}.k_L$) as shown in Fig. 8a. On the other hand, the Freundlich model [59] describes the multilayer adsorption process on heterogeneous adsorption sites, as described by a form of the Langmuir equation that varies as a function of the surface coverage. Freundlich model is expressed by Eq. (4):

$$\ln q_e = \ln k_F + \frac{1}{n} \ln C_e \tag{4}$$

where C_e is the equilibrium concentration of the adsorbate (mg/L), q_e is the amount of adsorbate adsorbed per unit

mass of adsorbent (mg/g). The affinity constant k_F (mg/g (l/mg)$^{1/n}$, relates to the adsorption capacity of the adsorbent and n is the constant where indicates the relative favourability of the adsorption process. Thus, a plot of $ln\ q_e$ vs. $ln\ C_e$ should be a straight line with a slope $1/n$ and an intercept of $ln\ k_F$ (Fig. 8b). Temkin model [60] assumes that the heat of adsorption of all the molecules in the layer decreases linearly with coverage due to adsorbent/adsorbate interactions, and adsorption is characterized by a uniform distribution of binding energies, up to some maximum binding energy. Temkin isotherm can be expressed in its linear form is expressed by Eq. (5):

$$q_e = B\ln k_T + B\ln C_e \quad (5)$$

A plot of q_e versus $ln\ C_e$ yielded a linear line enables to determine the isotherm constants k_T and B (Fig. 8c). k_T is the Temkin equilibrium binding constant (L/mg) that corresponds to the maximum binding energy, and constant B is related to adsorption heat. The adsorption heat of all the molecules in the layer is expected to decrease linearly with coverage because of adsorbate/adsorbate interactions. The isotherms related parameters were calculated, and the results are shown in Table 2. Among three tested models, the Freundlich described the adsorption system the best as reflected with the highest correlation coefficients, R^2 value (0.9299) compared with the Langmuir (0.9253), and Temkin (0.85558) models. This implied the multilayers coverage of MB has taken place on the ATRL surface. The ATRL surface is made up of small adsorption patches, which are energetically equivalent to each other in terms of adsorption phenomenon. Moreover, a value of $1/n > 1$ suggests weak adsorption bond between MB molecules onto ATRL surface. On the other side, a value of $1/n < 1$ suggests strong adsorption bond as a result of strong intermolecular attraction within the adsorbent layers. The value of n falls in the range of 2 to 10 indicates good adsorption. However, when the$n$ value falls between 1 to 2 indicates moderate adsorption capacity and value of n less than 1 indicating undesirable adsorption capacity. Thus, the value of n = 3.76 obtained from this work indicates beneficial adsorption. Thus, the monolayer adsorption capacity (q_{max}) for ATRL with MB was compared with other types of H_2SO_4 treated ligno-cellulosic materials as recorded in Table 3. ATRL shows a relatively high adsorption capacity for MB, where q_{max} was 263.2 mg/g, exceeding values reported for other biomass treated with H_2SO_4 activation for the uptake of MB.

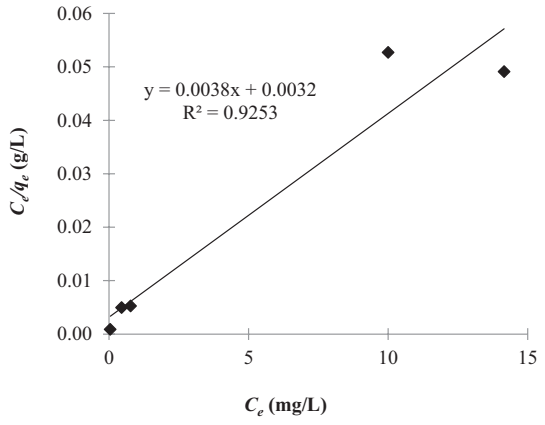

(a)

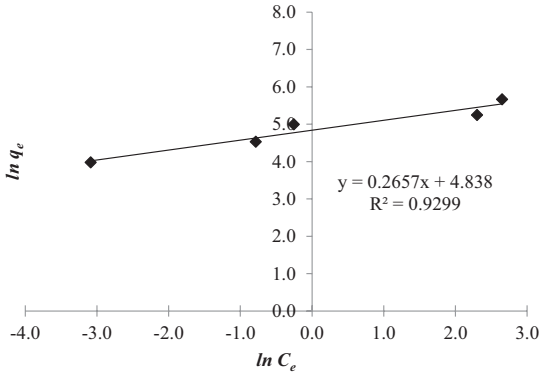

(b)

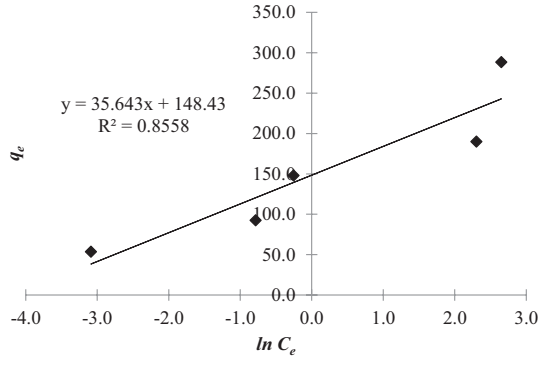

(c)

Fig. 8. Isotherm models for the adsorption of MB onto ATRL: (a) Langmuir, (b) Freundlich, and (c) Temkin

3.4. Adsorption kinetics

The pseudo-first-order model (PFO) and pseudo-second-order model (PSO) were used to investigate the

Table 2
Isotherm parameters for adsorption of MB by ATRL at 303 K

Isotherm	Parameters	Values
Langmuir	q_m (mg/g)	263.2
	k_L (L/mg)	1.19
	R^2	0.9253
Freundlich	K_F[(mg/g) (L/mg)$^{1/n}$]	126.22
	n	3.76
	R^2	0.9299
Temkin	B	35.64
	k_T(L/mg)	64.37
	R^2	0.8558

Table 3
Comparative of adsorption capacities for MB onto different biomass materials treated with H_2SO_4

H_2SO_4-treated biomass	Adsorbent dosage, g	pH	Temp. (K)	q_{max}(mg/g)	References
Rubber leaves	0.01 g/100 mL	5.6	303	263.2	This study
Pine-fruit shell	0.3 g/100 mL	8.5	298	529	[46]
Mango peels	0.14 g/100 mL	5~6	303	277.80	[36]
Coconut leaves	0.15 g/100 mL	6	303–323	126.90–149.30	[32]
Euphorbia rigida	0.2 g/100 mL	6	293–313	114	[41]
Bagasse	0.4 g/100 mL	9	300–333	49.8–56.5	[42]
Ficuscarica	0.5 g/100 mL	8	298–323	47.62	[48]
Parthenium hysterophorus	0.4 g/100 mL	7	298	39.7	[44]
Delonixregia pods	0.2 g/100 mL	7	298	23.30	[28]
Wild carrot	0.05 g/100 mL	6	298	21.00	[47]
Sunflower oil cake	0.2 g/100 mL	6	288–318	16.43	[45]

adsorption kinetics of MB dye on ATRL surface. The PFO was originally proposed by Lagergren [61] and its linearized form is given by Eq. (6):

$$\ln(q_e - q_t) = \ln q_e - k_1 t \tag{6}$$

where q_e is the amount of solute adsorbed at equilibrium per unit weight of adsorbent (mg/g), q_t is the amount of solute adsorbed at any time (mg/g), and k_1 is the adsorption constant. This expression is the most popular form of PFO model. k_1 values at different initial MB concentrations were calculated from the plots of *ln* $(q_e - q_t)$ vs. t (Fig. 9a) and the values are given in Table 4. The linear form of the PSO model is given by Eq. (7) [62]:

$$\frac{t}{q_t} = \frac{1}{k_2 q_e^2} + \frac{t}{q_e} \tag{7}$$

where, the PSO rate constant (k_2; g/mg min) and $q_{e,cal}$ were calculated from the intercept and slope of t/q_t vs. t, shown in Fig. 9b. In Table 4, the observed R^2 values are nearly unity ($R^2 \geq 0.99$) for the PSO kinetic model, where the values of $q_{e,cal}$ are in good agreement with $q_{e,exp}$. This suggests that the adsorption systems studied belong to the PSO kinetic model, based on the assumption that the rate-limiting step may be chemical adsorption (chemisorption).

3.5. Adsorption thermodynamics

Thermodynamic parameters provide further information about inherent energetic changes associated with adsorption process. The set of thermodynamic parameters of MB onto ATRL were determined by carrying out the adsorption experiments at 313, 323 and 333 K. Thermodynamic constants such as, standard Gibbs free energy change (ΔG°), standard enthalpy change (ΔH°) and standard entropy change (ΔS°) were calculated using the following equations [63]:

$$k_d = \frac{q_e}{C_e} \tag{8}$$

$$\Delta G^\circ = \Delta H^{\mathrm{O}} - T\Delta S^{\mathrm{O}} \tag{9}$$

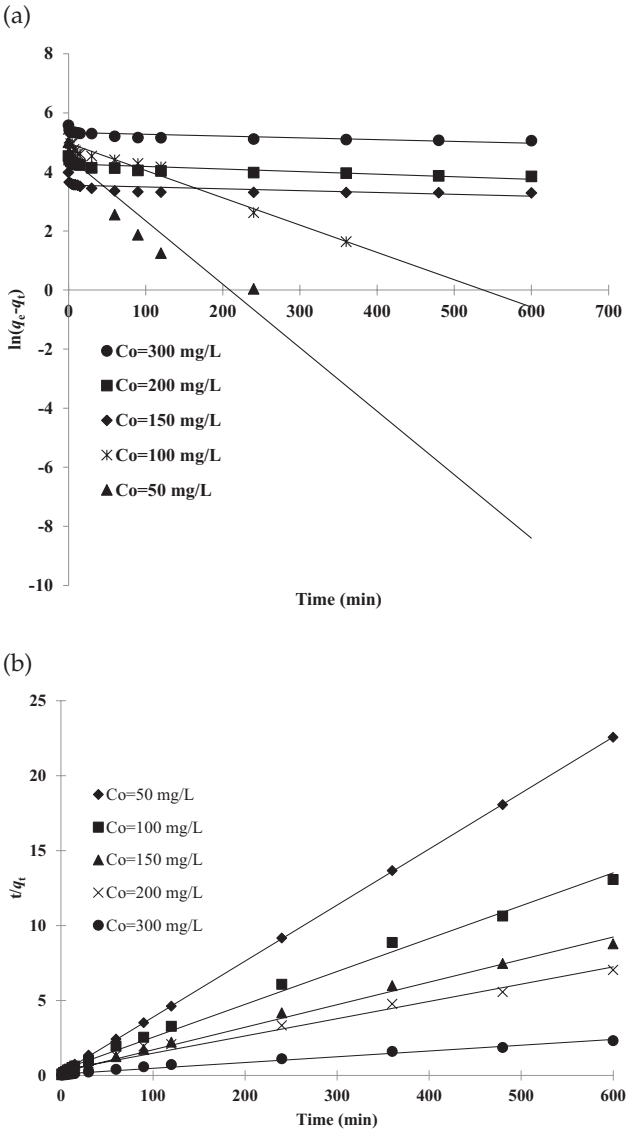

Fig. 9. Kinetic profiles for the adsorption of MB onto ATRL: (a) Pseudo-first-order (b) Pseudo-second-order.

Table 4
PFO and PSO kinetic parameters and their corresponding values at different initial dye concentrations by ATRL

Parameters	Concentration, C_o (mg/L)				
	50	100	150	200	300
$q_{e,exp}$ (mg/g)	53.40	92.51	147.77	188.92	288.24
PFO					
$q_{e,cal}$ (mg/g)	13.29	57.55	74.95	138.08	188.67
$k_{1\times10}{}^{-3}$ (1/min)	7.60	7.10	3.10	4.10	3.30
R^2	0.860	0.961	0.913	0.937	0.963
PSO					
$q_{e,cal}$ (mg/g)	53.48	93.46	147.06	188.68	285.71
$k_2 \times 10^{-4}$ (g/mg min)	51.73	6.13	2.94	1.42	1.03
R^2	1.000	0.999	0.995	0.993	0.992

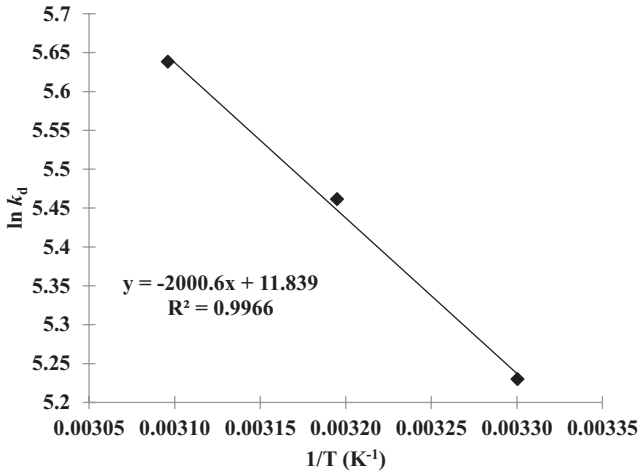

Fig. 10. Plot of ln k_d vs. 1/T for calculation of thermodynamic parameters for the adsorption of MB onto ATRL.

$$\ln k_d = \frac{\Delta S^\circ}{R} - \frac{\Delta H^\circ}{RT} \quad (10)$$

where k_d is the distribution coefficient, q_e is the concentration of MB adsorbed on ATRL at equilibrium (mg/L), C_e is the equilibrium concentration of MB in the liquid phase (mg/L), R is the universal gas constant (8.314J/mol·K) and T is the absolute temperature (K). The values of ΔH° and ΔS° were calculated from the slope and intercept of van't Hoff plots of lnk_d versus *1/T* respectively (Fig. 10). The thermodynamic parameters are listed in Table 5. In general, the negative values for ΔG° at all the studied temperature indicate that adsorption reaction is spontaneous process at high temperature, and not require any energy from an external source to uptake dye molecules onto ATRL surface [55]. A positive value of ΔH° suggests that the adsorption of MB onto ATRL surface is an endothermic in nature. A positive value of entropy change (ΔS°) implies an increased disorder at the solid/liquid interface during the adsorption process causing the adsorbate molecules (MB) to escape from the solid phase (ATRL surface) to the liquid phase. Therefore, the amount of MB molecules that can be adsorbed will increase by increasing the adsorption temperature.

Table 5
Thermodynamic parameters values for the adsorption of MB onto ATRL

Temperature (K)	Thermodynamics			
	k_d	ΔG° (kJ/mol)	ΔH° (kJ/mol)	ΔS° (J/molK)
303	373.53	–14.94	16.63	104.19
313	470.74	–15.98		
323	561.93	–17.02		

4. Conclusion

The research work clearly shows that carbonization of rubber leaf by H_2SO_4 activation provides a low-cost adsorbent for the removal of MB dye from aqueous solutions. The adsorption experiments indicated that the pseudo-second-order model provided the best description of the kinetic uptake properties, while adsorption results at equilibrium are described by the Langmuir model where the maximum adsorption capacity (q_{max}) is 263.2 mg/g. The thermodynamic parameters indicate that the adsorption process is an endothermic in nature and a spontaneous adsorption process. The results indicated that ATRL is an efficient adsorbent for MB adsorption.

References

[1] N.S.A. Mubarak, A.H. Jawad, W.I. Nawawi, Equilibrium, kinetic and thermodynamic studies of Reactive Red 120 dye adsorption by chitosan beads from aqueous solution, Energ. Ecol. Environ., 2 (2017) 85–93.
[2] A.H. Jawad, M.A.M. Ishak, A.M. Farhan, K. Ismail, Response surface methodology approach for optimization of color removal and COD reduction of methylene blue using microwave-induced NaOH activated carbon from biomass waste, Desal. Water Treat., 62 (2017) 208–220.
[3] A.H. Jawad, N.S.A. Mubarak, W.I. Nawawi, Optimization of sorption parameters for color removal of textile dye by cross-linked chitosan beads using Box- Behnken Design, MATEC Web of Conferences, 47 (2016) 05009.
[4] R. Juang, S. Swei, Effect of dye nature on its adsorption from aqueous solution onto activated carbon, Sep. Sci. Technol., 31 (1996) 2143–2158.
[5] A.H. Jawad, R.A. Rashid, R.M.A. Mahmuod, M.A.M. Ishak, N.N. Kasim, K. Ismail, Adsorption of methylene blue onto coconut (*Cocos nucifera*) leaf: optimization, isotherm and kinetic studies, Desal. Water Treat., 57 (2016) 8839–8853.
[6] A.H. Jawad, S. Sabar, M.A.M. Ishak, L.D. Wilson, S.S.A. Norrahma, M.K. Talari, A.M. Farhan, Microwave-assisted preparation of mesoporous activated carbon from coconut (*Cocos nucifera*) leaf by H_3PO_4-activation for methylene blue adsorption, Chem. Eng. Commun., 204 (2017) 1143–1156.
[7] A.H. Jawad, R.A. Rashid, K. Ismail, S. Sabar, High surface area mesoporous activated carbon developed from coconut leaf by chemical activation with H_3PO_4 for adsorption of methylene blue, Desal. Water Treat., 74 (2017) 326–335.
[8] A.R. Khataee, A. Movafeghi, S. Torbati, S.Y. SalehiLisar, M. Zarei, Phytoremediation potential of duckweed (*Lemna minor L.*) in degradation of C.I. Acid Blue 92: Artificial neural network modeling, Ecotoxicol. Environ. Saf., 80 (2012) 291–298.

[9] L. Fan, Y. Zhou, W. Yang, G. Chen, F. Yang, Electrochemical degradation of aqueous solution of Amaranth azo dye on ACF under potentiostatic model, Dyes Pigments, 76 (2008) 440–446.
[10] J.S. Wu, C.H. Liu, K.H. Chu, S.Y. Suen, Removal of cationic dye methyl violet 2B from water by cation exchange membranes, J. Membr. Sci., 309 (2008) 239–245.
[11] Y.S. Woo, M. Rafatullah, A.F.M. Al-Karkhi, T.T. Tow, Removal of Terasil Red R dye by using Fenton oxidation: a statistical analysis, Desal. Water Treat., 53 (2013) 1–9.
[12] A.H. Jawad, A.F.M. Alkarkhi, N.S.A. Mubarak, Photocatalytic decolorization of methylene blue by an immobilized TiO_2 film under visible light irradiation: Optimization using response surface methodology (RSM), Desal. Water Treat., 56 (2015) 161–172.
[13] A.H. Jawad, N.S.A. Mubarak, M.A.M. Ishak, K. Ismail, W.I. Nawawi, Kinetics of photocatalytic decolourization of cationic dye using porous TiO_2 film, J. Taibah Univ. Sci., 10 (2016) 352–362.
[14] F. Akbal, Adsorption of basic dyes from aqueous solution onto pumice powder, J. Colloid Interface Sci., 286 (2005) 455–458.
[15] A.H. Jawad, M.A. Islam, B.H. Hameed, Cross-linked chitosan thin film coated onto glass plate as an effective adsorbent for adsorption of reactive orange 16, Int. J. Biol. Macromolec., 95 (2017) 743–749.
[16] D. Cuhadaroglu, O.A. Uygun, Production and characterization of activated carbon from a bituminous coal by chemical activation, Afr. J. Biotechnol., 7 (2008) 3703–3710.
[17] J. Hayashi, A. Kazehaya, K. Muroyama A.P. Watkinson, Preparation of activated carbon from lignin by chemical activation, Carbon, 38 (2000) 1873–1878.
[18] J.R. Hernandez, F.L. Aquino, S.C. Capareda, Activated carbon production from pyrolysis and steam activation of cotton gin trash, Am. Soc. Agric. Biol. Eng., (2007) 1–8.
[19] X.J. Jin, Z.M. Yu, Y. Wu, Preparation of activated carbon from lignin obtained by straw pulping by KOH and K_2CO_3 chemical activation, Cellul. Chem. Technol., 46 (2010) 79–85.
[20] Y. Sun, J.P. Zhang, G. Yang, Z.H. Li, Removal of pollutants with activated carbon produced from K_2CO_3 activation of lignin from reed black liquors, Chem. Biochem. Eng Q., 20 (2006) 429–435.
[21] A.R. Yacob, Z.A. Majid, R.S.D. Dasril, V. Inderan, Comparison of various sources of high surface area carbon prepared by different types of activation, Malays. J. Anal Sci., 12 (2008) 264–271.
[22] Z. Zhu, A. Li, M. Xia, J. Wan, Q. Zhang, Preparation and characterization of polymer based spherical activated carbons, Chin. J. Polym. Sci., 26 (2008) 645–651.
[23] Z. Hu, M.P. Srinivasan, Mesoporous high-surface-area activated carbon, Micro Meso Mater., 43 (2001) 267–275.
[24] S. Guo, J. Peng, W. Li, K. Yang, L. Zhang, S. Zhang, Effects of CO_2 activation on porous structures of coconut shell-based activated carbons, Appl. Surf. Sci., 255 (2009) 8443–8449.
[25] J.N. Sahu, J. Acharya, B.C. Meikap, Optimization of production conditions for activated carbons from tamarind wood by zinc chloride using response surface methodology, Bioresour. Technol., 101 (2010) 1974–1982.
[26] J.M. Dias, M.C.M. Alvim-Ferraza, M.F. Almeida, J. Rivera-Utrilla, M. Sanchez-Polo, Waste materials for activated carbon preparation and its use in aqueous-phase treatment: a review, J. Environ. Manag., 85 (2007) 833–846.
[27] A.M. Khah, R. Ansari, Activated charcoal: preparation, characterization and applications: a review article, Int. J. Chem. Technol. Res., 1 (2009) 859–864.
[28] Y.S. Ho, R. Malaryvizhi, N. Sulochana, Equilibrium isotherm studies of methylene blue adsorption onto activated carbon prepared from *Delonix regia* pods, J. Environ. Prot. Sci., 3 (2009) 1–6.
[29] S. Idris, Y.A. Iyaka, B.E.N. Dauda, M.M. Ndamitso, M.T. Umar, Kinetic study of utilizing groundnut shell as an adsorbent in; removing chromium and nickel from dye effluent, Am. Chem. Sci. J., 2 (2012) 12–24.
[30] Z. Al-Qodah, R. Shawabkah, Production and characterization of granular activated carbon from activated sludge, Braz. J. Chem. Eng., 26 (2009) 127–136.
[31] J. Xu, L. Chen, H. Qu, Y. Jiao, J. Xie, G. Xing, Preparation and characterization of activated carbon from reedy grass leaves by chemical activation with H_3PO_4, Appl. Surface Sci., 320 (2014) 674–680.
[32] A.H. Jawad, R.A. Rashid, M.A.M. Ishak, L.D. Wilson, Adsorption of methylene blue onto activated carbon developed from biomass waste by H_2SO_4 activation: kinetic, equilibrium and thermodynamic studies, Desal. Water Treat., 57 (2016) 25194–25206.
[33] F. Marrakchi, M.J. Ahmed, W.A. Khanday, M. Asif, B.H. Hameed, Mesoporous activated carbon prepared from chitosan flakes via single-step sodium hydroxide activation for the adsorption of methylene blue, Int. J. Biol. Macromol., 98 (2017) 233–239.
[34] L. Gao, F. Dong, Q. Dai, G. Zhong, U. Halik, D. Lee, Coal tar residues based activated carbon: preparation and characterization, J. Taiwan Inst. Chem. Eng., 63 (2016) 166–169.
[35] R. Acosta, V. Fierro, A.M. Yuso, D. Nabarlatz, A. Celzard, Tetracycline adsorption onto activated carbons produced by KOH activation of tyre pyrolysis char, Chemosphere, 149 (2016) 168–176.
[36] A.H. Jawad, N.F.H. Mamat, M.F. Abdullah, K. Ismail, Adsorption of methylene blue onto acid-treated Mango peels: Kinetic, equilibrium and thermodynamic, Desal. Water Treat., 59 (2017) 210–219.
[37] Q.S. Liu, T. Zheng, N. Li, P. Wang, G. Abulikemu, Modification of bamboo-based activated carbon using microwave radiation and its effects on the adsorption of methylene blue, Appl. Surface Sci., 256 (2016) 3309–3315.
[38] Y. Gokce, Z. Aktas, Nitric acid modification of activated carbon produced from waste tea and adsorption of methylene blue and phenol, Appl. Surface Sci., 313 (2014) 352–359.
[39] H. Valdes, M. Sanchez-Polo, J. Rivera-Utrilla, C.A. Zaror, Effect of ozone treatment on surface properties of activated carbon, Langmuir, 18 (2002) 2111–2116.
[40] D. Pandey, 2002. Forest plantations working papers tropical forest plantation areas 1995 data set, in: M. Varmola, A. Del Lungo (Eds.), Working Paper FP/18 FAO, Rome, http://www.fao.org/DOCREP/005/Y7204E/ y7204e0b.htm#bm11.
[41] Ö. Gerçel, A. Özcan, A.S. Özcan, H.F. Gerçel, Preparation of activated carbon from a renewable bio-plant of *Euphorbia rigida* by H_2SO_4 activation and its adsorption behavior in aqueous solutions, Appl. Surf. Sci., 253 (2007) 4843–4852.
[42] L.W. Low, T.T. Teng, A. Ahmad, N. Morad, Y.S. Wong, A novel pretreatment method of lignocellulosic material as adsorbent and kinetic study of dye waste adsorption, Water Air Soil Pollut., 218 (2011) 293–306.
[43] H. Hasar, Adsorption of nickel (II) from aqueous solution onto activated carbon prepared from almond husk, J. Hazard. Mater., 97 (2003) 49–57.
[44] H. Lata, V.K. Garg, R.K. Gupta, Removal of a basic dye from aqueous solution by adsorption using *Parthenium hysterophorus*: An agricultural waste, Dyes Pigm., 74 (2007) 653–658.
[45] S. Karagöz, T. Tay, S. Ucar, M. Erdem, Activated carbons from waste biomass by sulfuric acid activation and their use on methylene blue adsorption, Bioresour. Technol., 99 (2008) 6214–6222.
[46] B. Royer, N.F. Cardoso, E.C. Lima, J.C.P. Vaghetti, R.C. Veses, Applications of Brazalin pine-fruit shell in natural and carbonized forms as adsorbents to removal of methylene blue from aqueous solutions: Kinetics and equilibrium study, J. Hazard. Mater., 164 (2009) 1213–1222.
[47] M. Mahadeva Swamy, B.M. Nagabhushana, R. Hari Krishna, Nagaraju Kottam, R.S. Raveendra, P.A. Prashanth, Fast adsorptive removal of methylene blue dye from aqueous solution onto a wild carrot flower activated carbon: isotherms and kinetics studies, Desal. Water Treat., 71 (2017) 399–405.
[48] D. Pathania, S. Sharma, P. Singh, Removal of methylene blue by adsorption onto activated carbon developed from *Ficus carica* bast, Arab. J. Chem., 10 (2017) S1445–S1451.
[49] N. Sharma, D.P. Tiwari, S.K. Singh, The efficiency appraisal for removal of malachite green by potato peel and neem bark: Isotherm and kinetic studies, Int. J. Chem. Environ. Eng., 5 (2014) 83–88.

[50] V.K. Garg, R. Kumar, R. Gupta, Removal of malachite green dye from aqueous solution by adsorption using agro-industry waste: a case study of *Prosopis cineraria*, Dyes Pigm., 62 (2004) 1–10.
[51] M.V. Lopez-Ramon, F. Stoeckli, C. Moreno-Castilla, F. Carrasco-Marin, On the characterization of acidic and basic surface sites on carbons by various techniques, Carbon, 37 (1999) 1215–1221.
[52] P. Barpanda, G. Fanchini, G.G. Amatucci, Structure, surface morphology and electrochemical properties of brominated activated carbons, Carbon, 49 (2011) 2538–2548.
[53] A.H. Jawad, M.A. Nawi, Characterizations of the photocatalytically-oxidized crosslinked chitosan-glutaraldehyde and its application as a sub-layer in the TiO_2/CS-GLA bilayer photocatalyst system, J. Polym. Environ., 20 (2012) 817–829.
[54] K.C. Bedin, A.C. Martins, A.L. Cazetta, O. Pezoti, V.C. Almeida, KOH-activated carbon prepared from sucrose spherical carbon: Adsorption equilibrium, kinetic and thermodynamic studies for Methylene Blue removal, Chem. Eng. J., 286 (2015) 476–484.
[55] R.A. Rashid, A.H. Jawad, M.A.M. Ishak, N.N. Kasim, KOH-activated carbon developed from biomass waste: adsorption equilibrium, kinetic and thermodynamic studies for Methylene blue uptake, Desal. Water Treat., 57 (2016) 27226–27236.
[56] M.C. Ncibi, B. Mahjoub, M. Seffen, Kinetic and equilibrium studies of methylene blue biosorption by *Posidonia oceanica (L.)* fibres, J. Hazard. Mater., 139 (2007) 280–285.
[57] S. Chakraborty, S. Chowdhury, P.D. Saha, Adsorption of Crystal Violet from aqueous solution onto NaOH modified rice husk, Carbohydr. Polym., 86 (2011) 1533–1541.
[58] I. Langmuir, The adsorption of gases on plane surfaces of glass, mica and platinum, J. Am. Chem. Soc., 40 (1918) 1361–1403.
[59] H. Freundlich, Ueber die adsorption in Loesungen (Adsorption in solution), Z. Phys. Chem., 57 (1906) 385–470.
[60] M.J. Temkin, V. Pyzhev, Recent modifications to Langmuir isotherms, Acta Physiochim. USSR, 12 (1940) 217–222.
[61] S. Lagergren, Zur theorie der sogenannten adsorption geloster stoffe, K. Sven. Vetenskapsakad. Handl., 24 (1898) 1–39.
[62] Y.S. Ho, G. McKay, Sorption of dye from aqueous solution by peat, Chem. Eng. J., 70 (1998) 115–124.
[63] G. Karaçetin, S. Sivrikaya, M. Imamoglu, Adsorption of methylene blue from aqueous solutions by activated carbon prepared from hazelnut husk using zinc chloride, J. Anal. Appl. Pyrolysis, 110 (2014) 270–276.